MULTIPLE PARAMETER MIXTURE FRACTION WITH TWO-STEP COMBUSTION CHEMISTRY FOR LARGE EDDY SIMULATION

Jason E. Floyd[1] & Kevin B. McGrattan[2]
[1]Hughes Associates, Inc. USA
[2]Building and Fire Research Laboratory, National Institute of Standards and Technology, USA

INTRODUCTION

A common approach for treating combustion in practical fire models is to use the mixture fraction, a conserved scalar to which all gas species can be related. Typically, infinitely fast chemistry is assumed, in which case the technique works well for fires scenarios in which there is an adequate supply of oxygen. A somewhat more complex approach is to create flamelet libraries that map temperature and mixture fraction to species mass fractions. This has been shown to work well in small scale simulations and is widely used in the combustion community. However, for simulations of fires in large structures, the inability to resolve flame temperatures and scalar dissipation rates, regardless of the turbulence model used, make detailed flamelet models impractical. Therefore, we seek a methodology that allows us to describe incomplete combustion and flame extinction at large scale while staying within the basic framework of the mixture fraction.

In the proposed new framework, the mixture fraction retains its classic definition as the mass fraction of gas that originates as fuel. However, with a single value of the mixture fraction it is not possible to account for products of incomplete combustion, or even the mixing of unburned fuel and oxygen. Instead, we need to decompose the mixture fraction into constitutive parts that represent the products of the different reactions. The number of components depends on the complexity of the phenomena. For example, to account for local flame extinction and also the production/destruction of CO, we need to decompose the mixture fraction into three components. This paper will document the new mixture fraction approach and test it against three sets of experimental data of varying scale: a slot burner, a hood experiment, and a compartment fire experiment. All three sets of experiments involve relatively clean burning fuels because the emphasis is on CO, not soot, production.

MATHATICAL FORMULATION

The combustion model in the Fire Dynamics Simulator (FDS), version 4,[1,2] uses only a single mixture fraction variable[3], defined in terms of the mass fractions, Y, molecular weights, W, and stoichiometric coefficients, ν, of the fuel and oxygen:

$$Z = \frac{sY_F - \left(Y_{O_2} - Y_{O_2}^{\infty}\right)}{sY_F^I - Y_{O_2}^{\infty}} \quad ; \quad s = \frac{\nu_{O_2} W_{O_2}}{\nu_F W_F} \qquad [1]$$

The superscripts, I and ∞, denote the fuel inlet and background values, respectively. Assuming infinitely fast chemistry, all gas species can be related to Z via a set of *state relations*. However, suppose we do not want to assume an infinitely fast, temperature-independent reaction of fuel and oxygen. How can the products of the complete and incomplete reactions be tied to the single variable, Z? They cannot – there are now additional degrees of freedom in the state relations.

Decomposing the Mixture Fraction

To overcome the limitations of the current single variable mixture fraction model, additional information is required to account for CO formation and extinction. To minimize the complexity of a new combustion model and to ensure its applicability to simulations with relatively coarse numerical grids, the simplest possible two-step CO formation mechanism is assumed[4]:

$$\text{Step 1: } \mathrm{F} + \mathrm{O}_2 \rightarrow \mathrm{CO} + \text{Other Products (i.e. } \mathrm{H}_2\mathrm{O} \text{ and Soot)} \qquad [2]$$

$$\text{Step 2: } \mathrm{CO} + \frac{1}{2}\mathrm{O}_2 \rightarrow \mathrm{CO}_2 \qquad [3]$$

Implicit in this formulation is the possibility that Step 1 does not occur at all; that is, fuel and oxygen can mix but not burn. This so-called "null" reaction, which could be considered Step 0, along with the two steps listed above, demands the inclusion in the model of three variables – one to account for the total amount of unburned fuel present (Step 0), one to account for the CO produced (Step 1), and one to account for the CO that has oxidized to form CO_2 (Step 2). Derivation of these variables starts with the transport equations, shown below, for fuel, CO, and CO_2. The subscripts 1 and 2 refer to the two steps shown above.

$$\frac{\mathrm{D}Y_\mathrm{F}}{\mathrm{D}t} = \nabla \cdot D\rho\nabla Y_\mathrm{F} + \dot{m}'''_{\mathrm{F},1}, \qquad [4]$$

$$\frac{\mathrm{D}Y_\mathrm{CO}}{\mathrm{D}t} = \nabla \cdot D\rho\nabla Y_\mathrm{CO} + \dot{m}'''_{\mathrm{CO},1} + \dot{m}'''_{\mathrm{CO},2} \qquad [5]$$

$$\frac{\mathrm{D}Y_{\mathrm{CO}_2}}{\mathrm{D}t} = \nabla \cdot D\rho\nabla Y_{\mathrm{CO}_2} + \dot{m}'''_{\mathrm{CO}_2,2}. \qquad [6]$$

The production and destruction rates of the species for Steps 1 and 2 are related via:

$$\frac{\dot{m}'''_{\mathrm{F},1}}{W_\mathrm{F}} = -\frac{\dot{m}'''_{\mathrm{CO},1}}{xW_\mathrm{CO}} \quad ; \quad \frac{\dot{m}'''_{\mathrm{CO},2}}{W_\mathrm{CO}} = -\frac{\dot{m}'''_{\mathrm{CO}_2,2}}{W_{\mathrm{CO}_2}} \qquad [7]$$

where x is the moles of CO formed per mole of fuel burned. Now define Z_1, Z_2, and Z_3:

$$Z_1 = Y_\mathrm{F}; \quad Z_2 = \frac{W_\mathrm{F}}{W_\mathrm{CO}x}Y_\mathrm{CO}; \quad Z_3 = \frac{W_\mathrm{F}}{xW_{\mathrm{CO}_2}}Y_{\mathrm{CO}_2}. \qquad [8]$$

Substituting Equations 7 and 8 into Equations 4 through 6, we obtain:

$$\frac{\mathrm{D}Z_1}{\mathrm{D}t} = \nabla \cdot D\rho\nabla Z_1 - \frac{W_\mathrm{F}\dot{m}'''_{\mathrm{CO},1}}{xW_\mathrm{CO}} \qquad [9]$$

$$\frac{\mathrm{D}Z_2}{\mathrm{D}t} = \nabla \cdot D\rho\nabla Z_2 + \frac{W_\mathrm{F}}{xW_\mathrm{CO}}\dot{m}'''_{\mathrm{CO},1} + \frac{W_\mathrm{F}}{xW_\mathrm{CO}}\dot{m}'''_{\mathrm{CO},2}. \qquad [10]$$

$$\frac{\mathrm{D}Z_3}{\mathrm{D}t} = \nabla \cdot D\rho\nabla Z_3 - \frac{W_\mathrm{F}}{xW_\mathrm{CO}}\dot{m}'''_{\mathrm{CO},2}. \qquad [11]$$

Note that the source terms for the three equations cancel by design. Thus, the sum of the three components is the mixture fraction:

$$Z_1 + Z_2 + Z_3 = Y_F + \frac{W_F}{xW_{CO}} Y_{CO} + \frac{W_F}{xW_{CO_2}} Y_{CO_2} = Z \qquad [12]$$

If we assume that water vapor and soot have yields that are fixed functions of CO and CO_2, then the three quantities Z_1, Z_2, and Z_3 can be used to determine the individual mass fractions of N_2, O_2, CO, CO_2, H_2O, soot, and unburned fuel. This is the precisely why the mixture fraction framework is used to track species; it reduces the number of transport equations that must be solved (in this case from 7 to 3). The process via which species are extracted from the mixture fraction parameters is discussed in the next section.

State Relations

The correspondence between the mixture fraction variables and the primitive species is known as the state relations. If a single mixture fraction variable is used in a calculation, it is easy, via a "look-up" table, to link individual gas mass fractions to the mixture fraction. However, for the above decomposition of the mixture fraction into three components, the state relations now become a function of three rather than one variable, and the computational "cost" of obtaining mass fractions during a calculation becomes significant. To reduce the computational expense, we construct a linear combination of state relations from the following three reaction pathways:

$$\text{Pathway 1:} \quad F + O_2 \rightarrow F + O_2 \ \text{(extinction / null reaction)} \qquad [13]$$

$$\text{Pathway 2:} \quad F + O_2 \rightarrow CO + \text{Other Products (CO formation / incomplete reaction)} \qquad [14]$$

$$\text{Pathway 3:} \quad F + O_2 \rightarrow CO_2 + \text{Other Products (CO destruction / complete reaction)} \qquad [15]$$

Pathway 1 is the so-called "null" or "Step 0" reaction. Pathway 2 is the same as Step 1 of the two-step reaction (Eq. 2). Pathway 3 is just Step 1 + Step 2 (Eq. 2 + Eq. 3). In some sense, every molecule that makes up the combustion products originated by way of one of the three pathways. For each pathway we can define a set of state relations. This is shown for methane in Figure 1. Note that for clarity water vapor and nitrogen are omitted and Z is limited to 0.5.

Figure 1 Methane state relations for the three reaction pathways (N_2 and H_2O omitted)

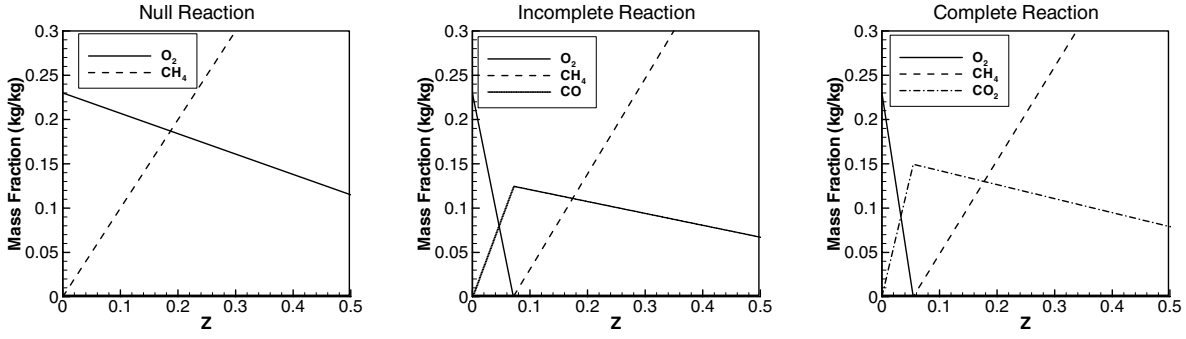

Since the state relations are piecewise-linear functions and since the above chemical reactions are linear expressions, it is postulated that the mass fractions of species can be given by linear combinations of the state relations. That is, the mass fraction of species i, Y_i, is given by:

$$Y_i(Z_1,Z_2,Z_3) = (1-c_{\mathrm{F}})\ Y_{i,1}(Z) + \ c_{\mathrm{F}}\left[(1-c_{\mathrm{CO}})\,Y_{i,2}(Z) + c_{\mathrm{CO}}\ Y_{i,3}(Z)\right], \qquad [16]$$

where c_{F} is a progress variable indicating the fraction of fuel that has not burned due to local flame extinction, c_{CO} is a progress variable indicating the fraction of CO that has been converted to CO_2, and the integer subscripts indicate the reaction pathway defined above. c_{CO} is given by:

$$c_{\mathrm{CO}} = \frac{1}{c_{\mathrm{F}}}\frac{Z_3}{Z_{3,\max}(Z)} \qquad [17]$$

where $Z_{3,max}$ is the maximum possible value of Z_3 (achieved when all the CO is oxidized). The progress variable related to fuel consumption is somewhat more complicated:

$$c_{\mathrm{F}} = \frac{Z - Z_1}{Z - Y_{\mathrm{F}}(Z)} \qquad [18]$$

$$Y_{\mathrm{F}}(Z) = \begin{cases} 0, & Z \le Z_f \\ \dfrac{Z - Z_f}{1 - Z_f}, & Z > Z_f \end{cases} \qquad [19]$$

$$Z_f = \left(1 + \frac{W_{\mathrm{O}_2}}{W_{\mathrm{F}}}\left(\frac{1}{Y^{\infty}_{\mathrm{O}_2}}\right)\left((1-c)\nu_{\mathrm{O}_2,2} + c\,\nu_{\mathrm{O}_2,3}\right)\right)^{-1} \qquad [20]$$

where c is a slightly different form of c_{co} needed to obtain the proper value of Z_f:

$$c = \frac{Z_3}{Z_2 + Z_3}. \qquad [21]$$

Figure 2 Methane State Relations for Pathway 2, Pathway 3, and $c = 0.5$ & $c_{\mathrm{F}} = 0$

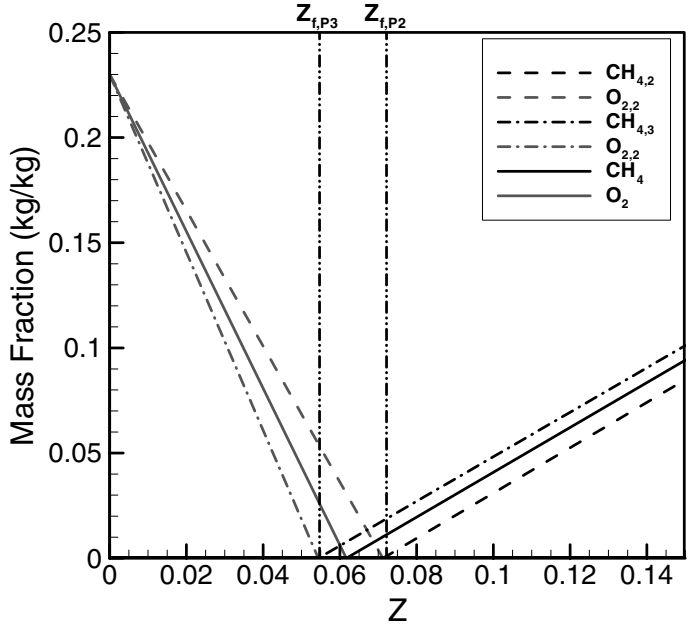

One additional step is required to obtain the mass fractions. Figure 2 shows the state relations for fuel and oxygen for Pathways 2 and 3 (dashed lines) along with a combination corresponding to $c = 0.5$ and $c_F = 0$ (solid lines). Note that above and below the stoichiometric values for Pathways 2 and 3 (vertical dashed lines), fuel and oxygen mass fractions are indeed simply linear combinations of their values from Pathways 2 and 3. However, in between the two stoichiometric values, simply taking a linear combination of the individual mass fractions would result in some oxygen surviving from Pathway 3 and some fuel surviving from Pathway 2. Since c_F is zero in this example (no extinction), fuel and oxygen cannot coexist. Therefore, in between the two stoichiometric values a correction is needed to account for the consumption of residual fuel and oxygen. This correction, $Y_{corr,i}$, is given by:

$$Y_{corr,i} = \begin{cases} c_{CO}\, s \dfrac{\nu_i W_i}{\nu_F W_F} Y_{F,3} & Z \le Z_f \\ (1 - c_{CO})\, s \dfrac{\nu_i W_i}{\nu_{O_2} W_{O_2}} Y_{O_2,2} & Z > Z_f \end{cases}, \qquad [22]$$

where s is -1 for reactants and +1 for products.

While the state relations appear complicated, it is important to remember that they simply serve to translate the mixture fraction variables back into species mass fractions. This is not the "combustion model," but rather an accounting procedure that allows us to solve half as many transport equations as we would otherwise have to do. While there is computational cost in translating the mixture fraction variables to species mass fractions, the cost is far less than that of solving the full set of transport equations. The combustion model is described next.

Combustion Model

The new combustion model implemented in FDS version 5 includes the two reaction steps described in Eqs. 2 and 3, along with the possibility of local extinction (Pathway 1). Transport equations are solved for the three components of the mixture fraction. At each time step of the calculation, the procedure described above is used to extract the individual species mass fractions from the mixture fraction variables. Then, an empirical criterion is used to decide whether or not Step 1, oxidation of fuel to CO and other products, can occur. If the temperature and oxygen mass fraction of a given cell and that of its neighbors are too low to support combustion (the black region of Figure 3), then Step 1 cannot occur. The neighboring cells represent either the fuel or oxidizer stream of classical diffusion flame theory. The local flammability criterion is based on the critical adiabatic flame temperature, as described by Beyler[5], and a simplified thermodynamic analysis by Mowrer[6]. The criterion determines if the energy released by consuming the maximum possible amount of oxygen can raise the local temperature above the critical flame temperature. If so, then Step 1 is allowed. Because large scale fire simulations usually have grid cell sizes far greater than the flame width, it is not appropriate to use a detailed kinetics model as the flame temperature and local strain rate are not available.

If the local environment is assumed to support combustion, Step 1 just depletes either fuel or oxygen, releasing the corresponding amount of energy into the grid cell, up to an empirically-based maximum value. This maximum value is based on two assumptions. First, that a flame sheet can generate no more than 200 kW/m^2 of energy[7]; second, that the numerical grid is resolved enough such that any grid cell is cut by only one flame sheet.

Figure 3 Flammability Criteria

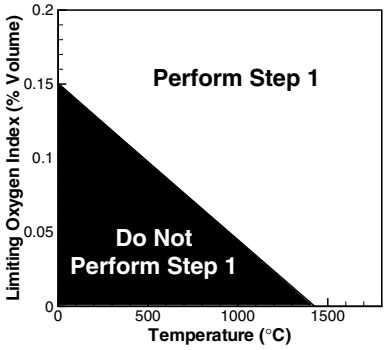

The limitation of this simple extinction model is that it is based on the conditions of the oxidizer stream, not the fuel stream. In other words, for any particular grid cell, an adequate oxygen supply in any of its neighboring cells automatically triggers Step 1 of the reaction to occur. In reality, low temperatures and/or low concentrations of fuel may still lead to flame extinction, but the model does not account for this. As will be discussed in the results section below, this means that the model may over-predict the burning rate and thus over-predict exhaust product concentrations in scenarios where fuel rich gases meet ambient air along an interface.

Step 2 of the reaction, the oxidation of CO, is determined by one of two methods depending on the outcome of Step 1. The first method presumes that if Step 1 results in any heat production in a given grid cell, then a flame (and flame temperatures) are present and the conversion of CO is "fast." For this case the maximum possible CO conversion is assumed, again limited by the upper bound on the local volumetric heat release rate. If no heat is produced in Step 1, it is presumed that a flame is not present and, therefore, the existing temperature is an accurate representation of the conditions in the cell. A finite rate computation[4] is then performed to determine the rate of CO oxidation. Oxidation of CO means that Z_2 becomes Z_3 using the source terms in Eq. 10 and Eq. 11.

A side benefit of the new combustion model is that it no longer requires the computation of the gradient of the mixture fraction normal to the flame sheet to determine the heat release rate. Past versions of FDS were susceptible to inaccuracies in the heat release rate because of this computation. Even though the transport algorithm is mass conserving globally, local numerical defects (known as "overshoots" and "undershoots") exist. These defects coincide with steep gradients and they led to unrealistically high and low local heat release rates. Attempting to correct both the numerical defects and the heat release rate often resulted in errors in the global heat release. The new mixture fraction formulation does not require the calculation of gradients, resulting in more accurate values of the local heat release rate and more flexibility in using "flux-correction" schemes to reduce the numerical defects in the transport algorithm.

VALIDATION

The new combustion model discussed above was implemented in FDS and tested against three sets of experimental measurements: a methane-air Wolfhard-Parker slot burner[8,9,10], selected Beyler hood experiments[11], and selected tests from the NIST reduced scale enclosure (RSE)[12].

Laminar Diffusion Flame from a Slot Burner

The Wolfhard-Parker slot burner consists of an 8 mm wide central slot flowing fuel surrounded by two 16 mm wide slots flowing dry air with 1 mm separations between the slots. The slots are 41 mm in length. The experimental errors have been reported as 5 % for temperature and 10 % to 20 % for the major species[9]. A 3D direct numerical simulation of one quarter of the burner with two symmetry planes was performed for the slot burner with a 0.5 mm grid resolution, 390,000 total grid cells. While the Wolfhard-

Parker burner is often discussed as a 2D flame, there are 3D effects that come into play when modeling the flame. In 2D, all computed quantities including radiation transport are mirrored at the symmetry boundary. Modeling the burner in 2D resulted in poorer predictions of temperature as radiant energy could not escape normal to the burner's axis. The post-flame CO was set to zero and the soot yield was also set to zero. The simulation was run for 4 s which took 104 hours on a single 2.4 GHz processor. While this seems a long time, it is noted that 0.5 mm grid resolution requires timesteps of 0.06 ms.

Figure 4 shows predicted and measured temperatures at three elevations above the burner. The model predicts a flame that is slightly narrower (5.5 mm vs. 6.5 mm or a 15 % error) and cooler (1700 °C vs. 1800 °C or a 5 % error) than measured. The model also predicts higher centerline temperatures. These results are not surprising. The new combustion model considers the first step, fuel to CO, to be infinitely fast, assuming that the local oxygen concentration satisfies the criteria of Figure 3. This is true in the vicinity of the lip of the burner. In reality, the cold fuel and air streams do not react infinitely fast there and some oxygen penetrates the flame at the base, resulting in cooler gases being entrained into the core of the flame with a resulting drop in the centerline temperature.

Figure 4. Predicted and measured temperature at three elevations (7 mm, 9mm and 11 mm) above a methane-air slot burner

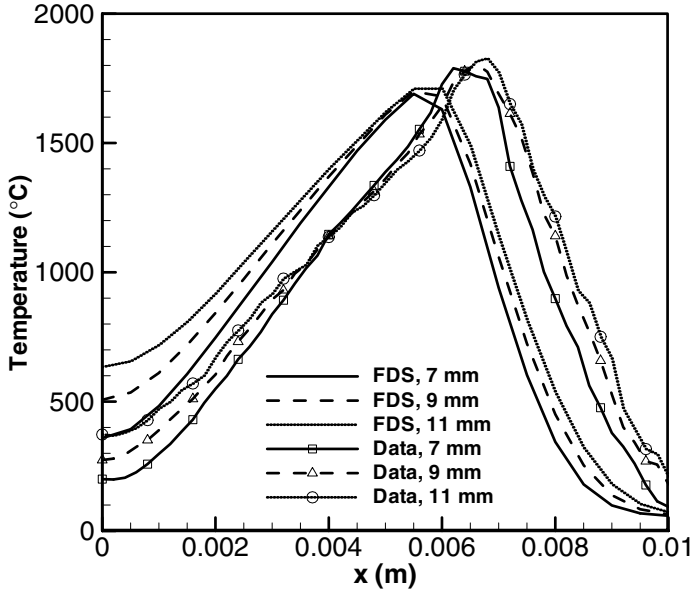

Figure 5 shows predicted and measured values of $CH_4 + O_2$, CO, CO_2 at three elevations above the burner along with a contour plot of CO near the burner lip (black rectangle is burner). Note that a small quantity of oxygen exists along the burner center per the observation made above. Along the centerline, the model predicts lower values of fuel and higher values of products than measured. The species profiles are also slightly narrower than measured, echoing the temperature plot in Figure 4. Again, this is likely due to the higher amounts of combustion at the burner lip resulting from the infinitely fast first step. The peak CH_4 values along the burner centerline have errors ranging from 6 % to 13 %, the peak CO_2 values in the flame have errors ranging from 3 % to 10 %, and the peak CO values in the flame have errors ranging from 9 % to 25 %. Given the reported 10 % to 20 % species measurement uncertainty, the new combustion model predicts well both the magnitude and shape of the mixture fraction profiles

The contour of CO illustrates the combustion model quite well. At the burner lip, fuel and oxygen first meet. Since ambient levels of oxygen exist on the air side of the slot and the temperatures are relatively low at the burner lip, combustion occurs and converts Z_1 to Z_2. This consumes the oxygen present and the CO does not have an opportunity to fully convert to CO_2. As the CO rises in the flame, oxygen is

entrained and the temperatures are high enough that the CO reacts with the entrained oxygen to form CO_2. Eventually, at a point high enough in the flame, all of the fuel is consumed and all of the CO is oxidized.

Figure 5. Predicted and measured mole fractions at three elevations (7 mm, 9mm and 11 mm) above a methane-air slot burner, along with contours of CO near the burner lip

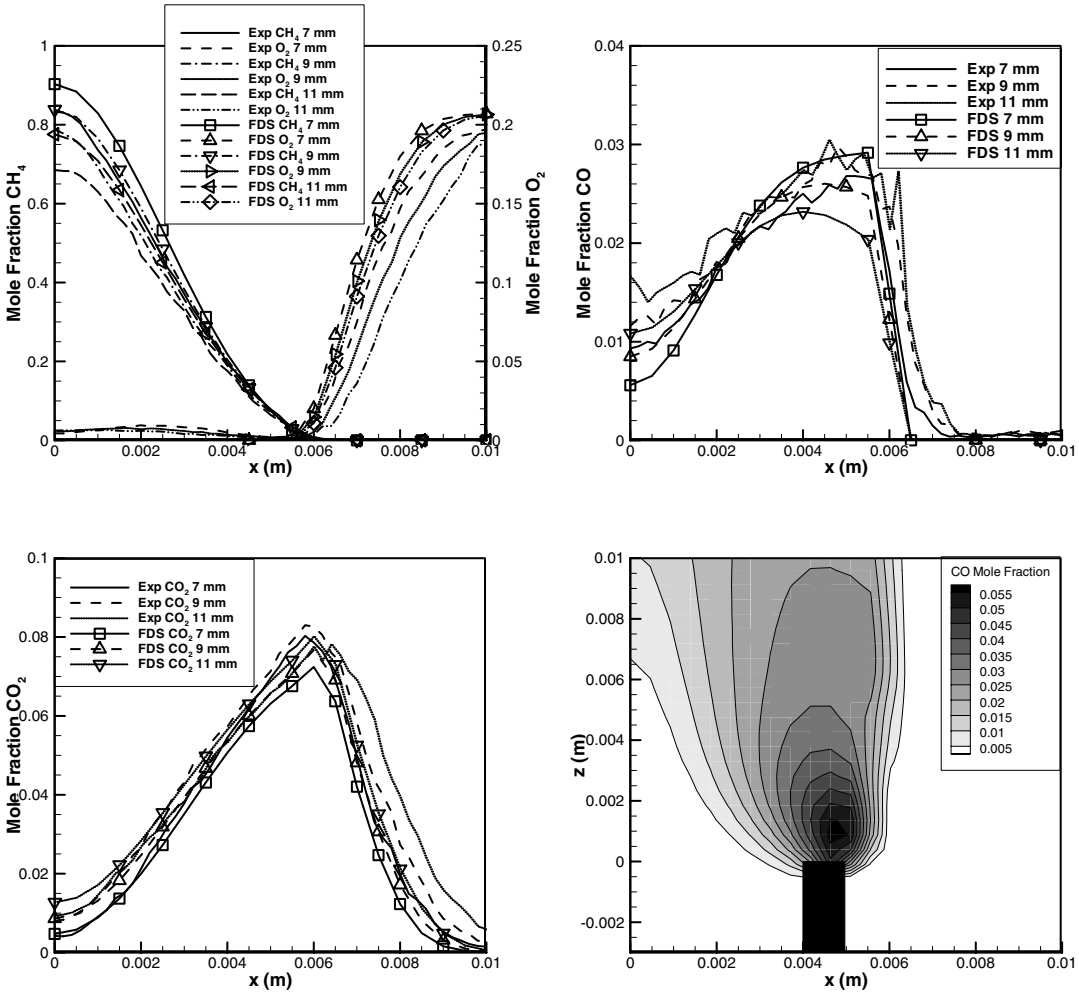

Beyler Hood Experiments

Beyler performed a large number of experiments involving a variety of fuels, fire sizes, burner diameters, and burner distances beneath a hood[11]. The hood consisted of concentric cylinders separated by a gap. The inner cylinder was shorter than the outer and this allowed combustion products to be removed uniformly from the hood perimeter. The exhaust gases were then analyzed to determine species concentrations. The burner could be raised and lowered with respect to the bottom edge of the hood. Based on the published measurement uncertainties, species errors are estimated at 6 %.

Simulations using the two step finite rate combustion model were performed for a number of the propane tests using a 19 cm burner. The cylindrical hood was transformed in the model into an equivalent area square box while preserving the height. A 1.4 cm grid was used with a total of 729,000 grid cells. As with the slot burner simulations, the first step was considered always infinitely fast and the second step was temperature dependent. It took 50 hrs to complete a 300 s simulation on a single 2.4 Gz processor.

Figure 6 shows species predictions made by the two step model compared with measured data for a range of fire sizes and burner positions. The dotted lines indicate the estimated measurement uncertainty. The model predicts the time-averaged species concentration at the hood exhaust vent. CO_2 predictions are

within the measurement uncertainty for all but one of the simulations performed. For the well-ventilated fires (-10 cm), CO, CO_2, and unburned fuel predictions match the data. As the fires become under-ventilated, CO is over-predicted while fuel and O_2 are under-predicted. The most likely explanation for the discrepancy is that the model assumes fuel and oxygen react infinitely fast in the vicinity of near ambient conditions. This occurs at the lower edge of the hood were the vitiated layer is adjacent to the ambient air below the hood, and as a result layer burning is occurring in the model which depletes the fuel and O_2 and creates CO. This is not unexpected, and indicates that more work is required to establish the conditions under which combustion in the first step, conversion of fuel to CO, will be allowed.

Figure 6. Comparison of measured and predicted species concentrations in the Beyler hood experiments, dotted lines show experimental uncertainty

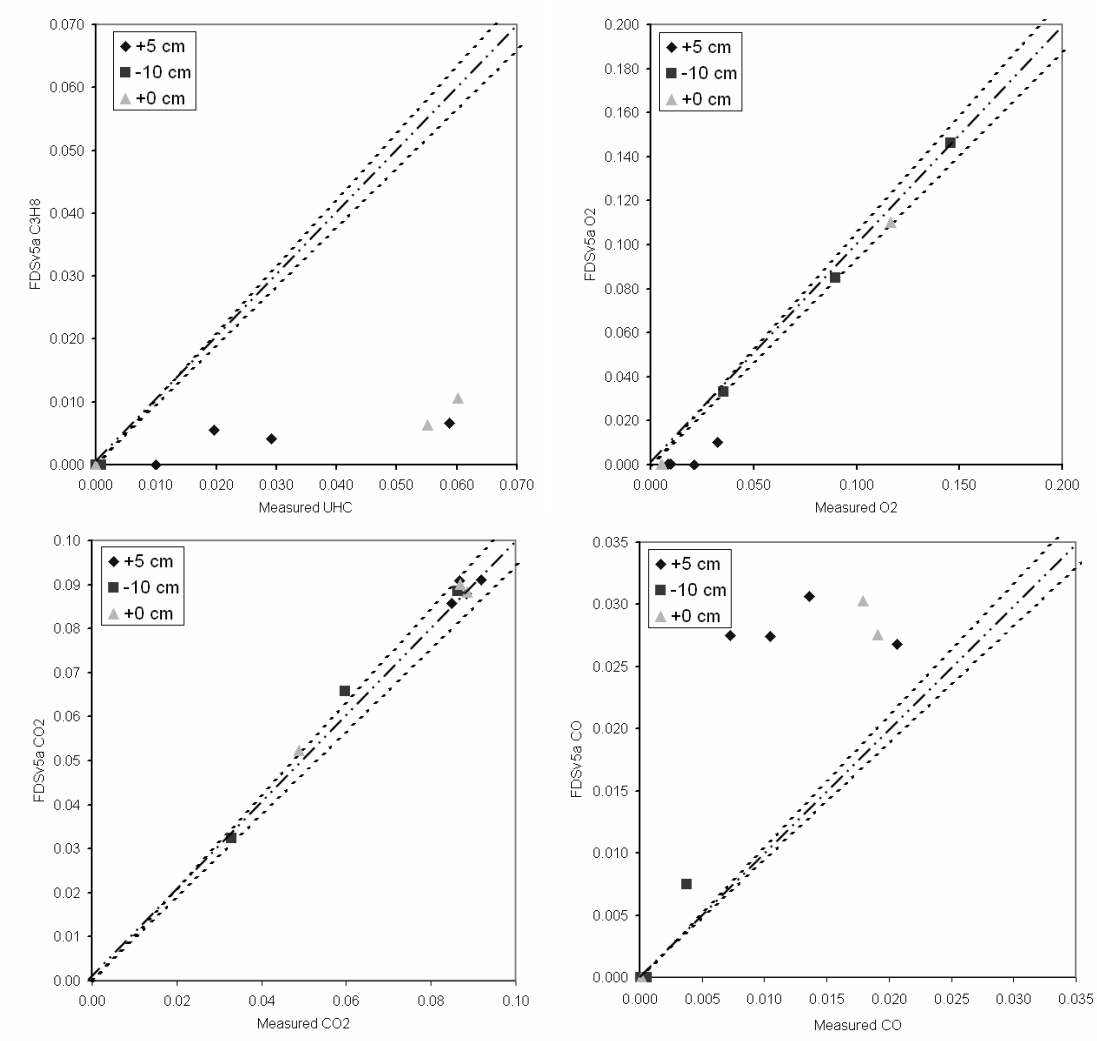

NIST Reduced Scale Enclosure

The NIST Reduced Scale Enclosure (RSE)[12] is a 40 % scaled version of the ISO 9705 compartment. It measures 0.98 m wide by 1.46 m deep by 0.98 m tall. The compartment contains a door centered on the small face that measures 0.48 m wide by 0.81 m tall. A 15 cm diameter natural gas burner was positioned in the center of the compartment. The burner was on a stand so that its top was 15 cm above the floor. Species measurements were made inside the upper layer of the compartment at the front near the door and near the rear of the compartment. The natural gas experiments were selected as currently the interest is in modeling CO production rather than CO and soot production.

Nine fire sizes were simulated: 50 kW, 75 kW, 100 kW, 150 kW, 200 kW, 300 kW, 400 kW, 500 kW, and 600 kW. The tests were modeled using properties of the natural gas supplied to the test facility[13,14]. The model geometry included the compartment interior along with a 0.6 m deep region outside the door that was modeled using a 2.4 cm grid resolution for a total of 240,000 grid cells. The wall boundary condition used a reduced material density for the compartment lining. This was done so that the computation would reach steady state in less time. Each fire size was simulated for 300 s which took approximately 45 hours on a 2.4 GHz processor.

Figure 7 shows the measured and predicted CO_2 and CO concentrations. The measured values are from the test series performed Bryner, Johnsson, and Pitts[12]. The model matches the data up to a fire size of 300 kW, including the location of the peak CO_2 concentration at 200 kW. For larger fires the model predicts more CO surviving in the upper layer than measured, along with correspondingly lower CO_2 levels. At 300 kW the model predicts front and rear concentrations of 7.7 % and 7.4 % CO_2 vs. 7.5 % and 7.7 % in the data. At 600 kW the respective CO_2 values are 6.5 % and 5.3 % vs. 6.1 % and 6.8 % in the data. For CO at 300 kW the model predicts 2.2 % and 2.4 % vs. 1.8 % and 2.0 % in the data. For CO at 600 kW the model predicts 3.2 % and 3.8 % vs. 2.9 % and 2.1 % in the data. As the compartment becomes under-ventilated, the model under-predicts CO_2 and over-predicts CO. The relative error increases as the compartment becomes more under-ventilated. However, note that the absolute model under-prediction of CO_2 in the rear (1.5 %) is equivalent to the absolute over-prediction of CO (1.7 %). This implies that part of the model error results from the assumption of infinitely fast chemistry for the first step. Furthermore, since the model as implemented performs the two steps sequentially, higher CO is predicted where the first step consumes all of the available oxygen.

Figure 7 Predicted and measured CO_2 and CO concentrations for the NIST RSE experiments of Bryner, Johnsson, and Pitts[12]

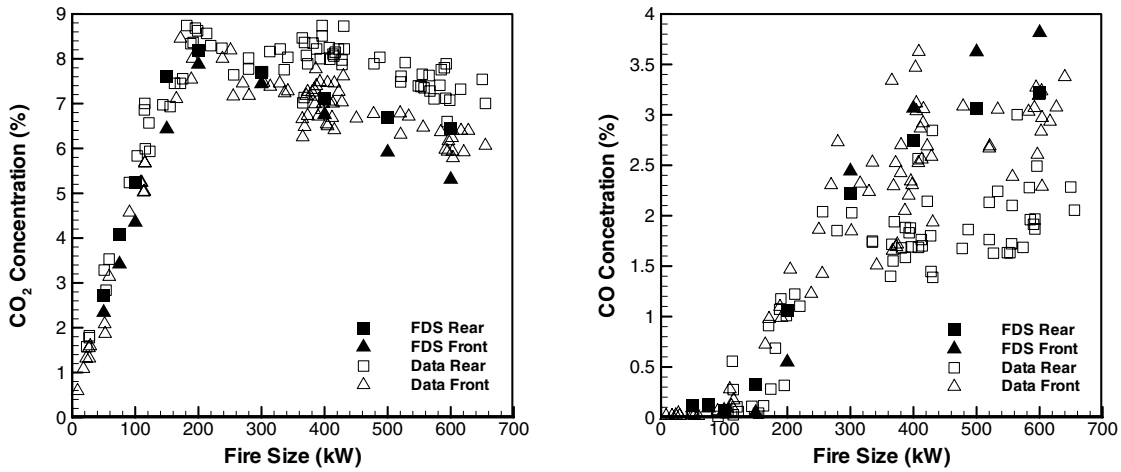

CONCLUSIONS

A combustion model based on a multiple parameter mixture fraction has been developed to account for local extinction and incomplete combustion, in particular, the formation and destruction of carbon monoxide. The new model was used to simulate three sets of experiments. The first experiment was a methane-air slot burner. The model successfully predicted the peak CO concentration as a function of elevation within the flame with errors ranging from 6 % to 25 % of the measurements and the overall flame temperature 5 % of the measurements. This is compared to experimental uncertainties of 10 % to 20 % for species and 5 % for temperatures. Since the current implementation of the two-step model assumes the first step is infinitely fast, it predicted a slightly narrower flame as combustion occurred at the burner lip rather than at a slight stand-off distance. The second set of experiments, conducted by Beyler, was designed to create a vitiated fire environment under a small hood. Predictions of species concentrations for the well-ventilated experiments correlate very well with the data (within the

experimental uncertainty of 6 %). For the higher equivalence ratio experiments, the model under-predicts fuel and oxygen and over-predicts CO. This appears to be a result of the model not being able to predict extinction at the base of the hood. The final set of experiments was a set of reduced-scale enclosure fires at NIST. The new model generally matched the trends seen in the data, though with an approximately 1 % to 2 % by volume error in the CO (relative error of 10 % to 80 %) and CO_2 (relative error of 10 % to 20 %) predictions for the under-ventilated fires. Overall, the validation results indicate that the new method tends to over-predict CO formation because of its assumption that the first step of the reaction is infinitely fast.

There is room for improvement to the current approach while remaining within the developed mixture fraction framework. A better method of determining when to allow the first step of the reaction to occur should result in improved predictions of CO formation. It is also noted that the current mixture fraction framework could be extended to a fourth parameter that could be used for tracking soot formation. However, a point of diminishing returns is reached as the number of mixture fraction variables approaches the number of primitive species, defeating the purpose of the mixture fraction approach.

ACKNOWLEDGEMENTS

The first author is supported by the Building and Fire Research Laboratory of the National Institute of Standards and Technology via its Fire Grants Program.

REFERENCES

[1] McGrattan, K., Hostikka, S., Floyd, J., Baum, H. and Rehm, R. 2007 *Fire Dynamics Simulator (Version 5): Technical Reference Guide*. NIST SP 1018-5. Gaithersburg, MD: National Institute of Standards and Technology.

[2] McGrattan, K., Klein, B., Hostikka, S., and Floyd, J. 2007. *Fire Dynamics Simulator (Version 5): User's Guide*. NIST SP 1019-5. Gaithersburg, MD: National Institute of Standards and Technology.

[3] Floyd, J., McGrattan, K., Hostikka, S., and Baum, H., 2003. CFD Fire Simulation Using Mixture Fraction Combustion and Finite Volume Radiative Heat Transfer, *Journal of Fire Protection Engineering,* **13** (1), pp.11-36.

[4] Westbrook, C. and Dryer, F., 1981. Simplified Reaction Mechanisms for the Oxidation of Hydrocarbon Fuels in Flames, *Combustion Science and Technology*, **27**, pp.31-43.

[5] Beyler, C., 2002. Flammability Limits of Premixed Diffusion Flames. In DiNenno, P., ed. *Handbook of Fire Protection Engineering*, 3rd ed. Quincy, MA: National Fire Protection Association.

[6] Mowrer, F., 2002. Private communication.

[7] Linteris, G. and Rafferty, I. 2003. Scale Model Flames for Determining the Heat Release Rate from Burning Polymers, *Fourth International Symposium on Scale Modeling (ISSM-IV)*.

[8] Smyth, K., 1999. *Fire Experimental Results*. [online]. Available from: http://fire.nist.gov/fire/flamedata [cited on 6 June 2007].

[9] Norton, S., Smyth, K., Miller, J., and Smooke, M., 1993. Comparison of Experimental and Computed Species Concentration and Temperature Profiles in a Laminar Two-Dimensional, Methane/Air Diffusion Flame, *Combustion Science and Technology*, **90**, pp.1-34.

[10] Smyth, K., 1996. NO Production and Destruction in a Methane/Air Diffusion Flame, *Combustion Science and Technology*, **155**, pp.151-176.

[11] Beyler, C., 1986. Major Species Production by Diffusion Flames in a Two-Layer Compartment Fire Environment, *Fire Safety Journal*, **10**(1), pp.47-56.

[12] Bryner, N., Johnsson, E., and Pitts, W., 1994. *Carbon Monoxide Production in Compartment Fires – Reduced-Scale Test Facility*. NISTIR 5568. Gaithersburg, MD: National Institute of Standards and Technology.

[13] Bundy,M., Hamins, A., Johnsson, E., Kim, S., Ko, G., and Lenhert, D. 2007. *Measurements of Heat and Combustion Products in Reduced-Scale Ventilation-Limited Compartment Fires.* NIST Technical Note TN-1483 (in internal review). Gaithersburg, MD: National Institute of Standards and Technology.

[14] Jonsson, E., Bundy, M. and Hamins, A. 2007 Reduced-Scale Enclosure Fires – Heat and Combustion Product Measurements. *Interflam 2007*. London, England. Interscience Communications.